21

Ab Initio Studies of H-Bonded Systems: The Cases of Ferroelectric KH_2PO_4 and Antiferroelectric $NH_4H_2PO_4$

S. Koval[1], J. Lasave[1], R. L. Migoni[1], J. Kohanoff[2] and N. S. Dalal[3]
[1]*Instituto de Física Rosario, Universidad Nacional de Rosario, CONICET*
[2]*Atomistic Simulation Group, The Queen's University, Belfast*
[3]*Department of Chemistry and NHMFL, Florida State University*
[1]*Argentina*
[2]*United Kingdom*
[3]*USA*

1. Introduction

A wide variety of molecular compounds are bound by Hydrogen bridges between the molecular units. In these compounds cooperative proton tunneling along the bridges plays an important role.(1) However, it is apparent that not only the proton behavior is relevant but also that of their associated matrix, leading to a wide range of possible behaviors. We are thus faced with the consideration of two in principle coupled subsystems: the proton tunneling subunit and the host lattice. Ubbelhode noted, in 1939,(2) that the nature of the H-bond changes upon substitution of Deuterium (D) for H. In addition, many H-bonded compounds show structural transitions that are strongly affected by deuteration.(3) The common assumption that proton tunneling completely dominates the transitional physics, in a chemically and structurally unchanged host, is an oversimplified model. Since the 1980's, a number of authors have noted in pressure studies that the changes in transition temperatures correlate well with the H-bond parameters.(4) Thus, the proton's (deuteron's) dynamics and the host are mutually determined. The host-and-tunneling system is not separable, and the physics of the proton-tunneling systems must be revised.(5)

Typical examples are KH_2PO_4 (KDP) and its analogs.(6) They were discovered as a novel family of ferroelectric (FE) compounds in the late 1930's by Busch and Scherer.(7) It was shown that KDP undergoes a paraelectric (PE) to FE transition at a critical temperature of ≈ 123 K. It was also found that upon substitution of Ammonium for Potassium the resulting $NH_4H_2PO_4$ (ADP) becomes antiferroelectric (AFE) below $T_c = 148$ K,(8) although chemically the NH_4^+ ion usually behaves similarly to the alkali metal ions, in particular K^+ and Rb^+. The structures of the AFE phase of ADP and the FE phase of KDP are depicted schematically from a top view in Fig. 1(a) and Fig. 1(c), respectively. Both materials exhibit strong H $\rightarrow$ D isotope effects on their transition temperatures. In subsequent years KDP and ADP have found extensive applications in electro-optical and laser spectroscopy. Nowadays, they are widely used in controlling and modulating the frequency of laser radiation in optoelectronic

devices, amongst other uses such as TV screens, electro-optic deflector prisms, interdigital electrodes, light deflectors, and adjustable light filters.(6) Besides the technological interest in these materials, they were also extensively studied from a fundamental point of view. KDP is considered the prototype FE crystal for the wide family of the H-bonded ferroelectric materials, while ADP is the analogous prototype for the AFE crystals belonging to this family. What makes these materials particularly interesting is the possibility of growing quite large, high-quality single crystals from solution, thus making them very suitable for experimental studies. Indeed, a large wealth of experimental data has been accumulated during second half of the past century. (4; 6; 9–13)

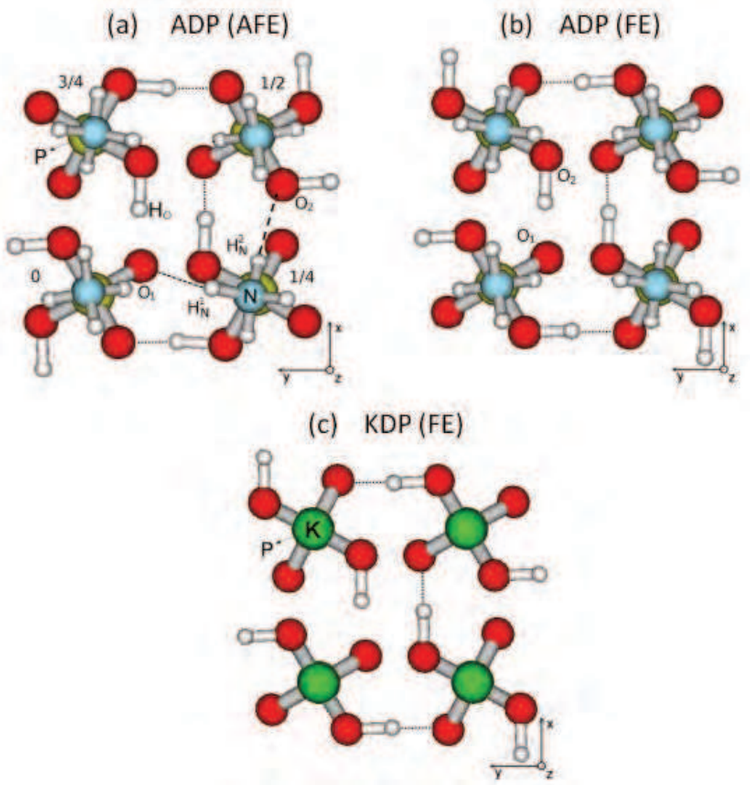

Fig. 1. Schematic representation of (a) AFE phase of ADP, (b) hypothetical FE phase in ADP, and (c) FE phase of KDP. The structures are shown from a top (z-axis) view. Acid H-bonds are shown by dotted lines while in case (a) short and long N-H$\cdots$O bonds are represented by short-dashed and long-dashed lines, respectively. Fractional z coordinates of the phosphate units are also indicated in (a).

The phosphates in KDP and ADP are linked through approximately planar H-bonds forming a three-dimensional network. In the PE phase at high temperature, hydrogens occupy with equal probability two symmetrical positions along the H-bond separated a distance δ (Fig. 2), characterizing the so-called disordered phase. Below the critical temperature in both compounds, hydrogens fall into one of the symmetric sites, leading to the ordered FE phase in KDP (see Fig. 2 and Fig. 1(c)), or the AFE phase in ADP (Fig. 1(a)). In KDP the spontaneous polarization P_s appears perpendicular to the proton ordering plane (see Fig. 2), the PO_4 tetrahedra becoming distorted. In ADP, there is an ordered AFE phase with dipoles pointing

in alternating directions along chains in the basal plane (Fig. 1(a)). In both cases, each PO_4 unit has two covalently bonded and two H-bonded hydrogens, in accordance with the well-known ice rules. The oxygen atoms that bind covalently to the acid H are called donors (O_2 in Figs. 1 and 2), and those H-bonded are called acceptors (O_1 in Figs. 1 and 2).
The proton configurations found around each phosphate in the AFE and FE phases of ADP and KDP, respectively, are essentially different, as depicted in Fig. 1(a) and Fig. 1(c). The low-temperature FE phase of KDP is characterized by local proton configurations around phosphates called *polar*, with electric dipoles and a net spontaneous polarization pointing along the z direction (Fig. 1(c)). There are two possible polar configurations which are built with protons attached to the bottom or the top oxygens in the phosphate, and differ in the sign of the corresponding dipoles along z. These are the lowest-energy configurations realized in the FE phase of KDP. On the other hand, the low-temperature AFE phase of ADP has local proton arrangements in the phosphates called *lateral*. In fact, these configurations have two protons laterally attached to two oxygens, one at the top and the other at the bottom of the phosphate units (Fig. 1(a)). There are four possible lateral configurations, which yields four different orientations of the local dipoles along the basal plane. Another important feature of the ADP structure is the existence of short and long N-H$\cdots$O bonds in the AFE phase, which link the ammonium with different neighboring phosphates (Fig. 1(a)).

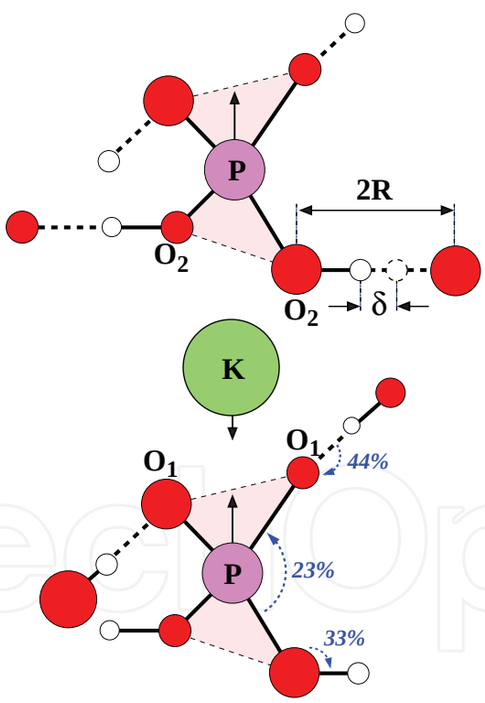

Fig. 2. Schematic lateral view of the atomic motions (solid arrows) happening upon off-centering of the H-atoms which correspond to the FE mode pattern in KDP. Also shown are the concomitant electronic charge redistributions (dotted curved arrows) and the percentages of the total charge redistributed between different orbitals and atoms.

Although considerable progress has been made during the last century, a complete understanding of the FE and AFE transition mechanisms in KDP and ADP is still lacking. The six possible proton configurations obeying the ice rules observed in the low-temperature

phases of KDP and ADP, polar and lateral arrangements respectively, were considered earlier by Slater to develop an order-disorder local model for the phase transition in KDP. (14) Slater assigned energies 0 and $\epsilon_s > 0$ to the polar and lateral configurations respectively in his model for KDP, and predicted a sharp first-order FE transition. But because it is a static model in its original form, it is difficult to use it for understanding, in particular, dynamic properties, such as electric transport and related protonic hopping in the low temperature FE phase. (15) Takagi improved the theory by including the possibility of configurations with one or three protons attached to the phosphate (Takagi configurations) with energy ϵ_t per phosphate, which is well above those of the polar and lateral configurations. (16) These configurations violate the ice rules and arise, e.g., when a proton from a H-bond common to two polar states moves to the other bond side. This leads to the formation of a Takagi-pair defect in two neighboring phosphates that finally remain with one and three protons. (17) The Takagi defects, which are the basic elements of domain walls between regions of opposite polarization, may propagate throughout the lattice and are relevant for the dynamic behavior of the system. (15)

On the other hand, a modification of the original order-disorder Slater model,(14) with a negative Slater energy $\epsilon_s < 0$ proposed by Nagamiya, was the first explanation of antiferroelectricity in ADP. (18) This model favors the AFE ordering of lateral protonic configurations in the O-H$\cdots$O bridges, with dipoles along the basal plane, over the FE ordering of polar configurations with dipoles oriented in the z direction in ADP (see the schematic representation of the hypothetical FE state in ADP, Fig. 1(b)). However, this alone is insufficient to explain antiferroelectricity in ADP. Actually, FE states polarized in the basal plane, not observed experimentally, have energies comparable to the AFE one.(19–21) Ishibashi *et al*. introduced dipolar interactions in a four-sublattice version of the Slater model to rule them out and predicted the observed first-order AFE transition.(19; 20) Although the general characteristics of the AFE transition are well explained by their theory, the transversal and longitudinal dielectric properties are not consistently determined. Using an extended pseudospin model that takes into account the transverse polarization induced by the proton displacements along the H-bonds, Havlin *et al.* were able to explain successfully the dielectric-constant data.(22) The above model explanation of the AFE proton ordering in the low-temperature phase of ADP (Fig. 1(a)) was confirmed by neutron diffraction measurements.(23) Based on that structural data, Schmidt proposed an effective interaction of acid protons across the NH_4^+ ion providing the needed dipolar coupling that leads to the AFE ordering. Although there is no clear microscopic justification for that specific interaction, this model led to successful mean field simulations for ADP and the proton glass $Rb_{1-x}(NH_4)_xH_2PO_4$.(15; 24)

Strong experimental evidence for the coexistence of the FE and AFE domains as T approaches the AFE transition from above has been obtained in EPR studies on ADP using the $(AsO_4)^{4-}$ radical as probe.(25; 26) This suggests that the FE state (Fig. 1(b)) is very close to the AFE ground state (Fig. 1(a)), but there has been no further theoretical justification. Within a model view, a delicate balance between the bare Slater energy and the dipolar interactions would favor one of them.(20)

The strong H $\rightarrow$ D isotope effects exhibited by these materials on their FE or AFE transition temperatures (the critical temperature T_c nearly doubles in the deuterated compounds)(6) are still being debated. This giant effect was first explained by the quantum tunneling model proposed in the early sixties. (27) Within the assumption of interacting, single-proton double wells, this model proposes that individual protons tunnel between the two wells. Protons

have a larger tunnel splitting and are more delocalized than deuterons, thus favoring the onset of the disordered PE phase at a lower T_c. Improvements of the above model to explain the phase transition in KDP include coupling between the proton and the K-PO_4 dynamics. (28–33) These models have been validated *a posteriori* on the basis of their predictions, although there is no direct experimental evidence of tunneling. Only very recent neutron Compton scattering experiments seem to indicate the presence of tunneling.(34) However, the connection between tunneling and isotope effect remains unclear, in spite of recent careful experiments.(35)

On the other hand, a series of experiments carried out since the late eighties (4; 36–40) provided increasing experimental evidence that the geometrical modification of the H-bonds and the lattice parameters upon deuteration (Ubbelohde effect (2)) is intimately connected to the mechanism of the phase transition. The distance δ between the two collective equilibrium positions of the protons (see Fig. 2) was shown to be remarkably correlated with T_c.(4) Therefore, it seems that proton and host cage are connected in a non-trivial way, and are not separable.(5) These findings stimulated new theoretical work where virtually the same phenomenology could be explained without invoking tunneling. (41–45) However, these theories were developed at a rather phenomenological level.

Because of the fundamental importance of the FE and AFE phenomena, as well as from the materials-engineering point of view, it was desirable to carry out quantum mechanical calculations at the first principles (ab initio) level to understand the transition mechanism as well as the isotope effects on the various properties of these materials. These approaches have the advantage of allowing for a confident and parameter-free analysis of the microscopic changes affecting the different phases in these H-bonded FE and AFE compounds. Such an enterprise has recently been possible via the availability of efficient algorithms and large-scale computational facilities. Thus we have carried out ab-initio quantum-theoretical calculations on KDP, (17; 46–48) with particular emphasis on the H $\rightarrow$ D isotope effect in the ferroelectric transition temperature T_c, that shifts from 123 K in KDP to 224 K on deuteration.(6) It was found that the T_c-enhancement can be ascribed to tunneling, but with an additional feed-back effect on the O-H$\cdots$O potential wells.(47; 48)

Encouraged by the KDP results, we undertook a similar study on ADP, (21) because ADP and its analogous AFE compounds such as $NH_4H_2AsO_4$ (ADA) and their deuterated analogues have received much less attention than KDP.(6; 15) Thus how the presence of the NH_4^+ units renders antiferroectricity to ADP and ADA has not been well understood.(15; 18–20) Our *ab initio* results showed that the optimization of the N-H$\cdots$O bonds and the accompanying NH_4^+ distortions lead to the stabilization of the AFE phase over the FE one in ADP.(21)

The purpose of the present contribution is to review and discuss the fundamental behavior of the FE and AFE H-bonded materials KDP and ADP, as explained by our recent first-principles calculations. The following questions are addressed: (i) What is the microscopic mechanism leading to ferroelectricity in KDP and antiferroelectricity in ADP?, (ii) What is the quantum mechanical explanation of the double-site distribution observed in the PE phases of KDP and ADP?, (iii) How does deuteration produce geometrical effects?, (iv) What is the main cause of the giant isotope effect: tunneling, the geometrical modification of the H-bonds, or both?

In the next Section 2 we provide details of the methodology and approximations used. Section 3 is devoted to the ab initio results. In Subsection 3.1 we present and compare the structural results with the available experimental data for both KDP and ADP. In Subsection 3.2 we describe the electronic charge flows involved in the instabilities of the systems. The question,

why ADP turns out to be antiferroelectric, in contrast to KDP, is analyzed in Subsection 3.3. Subsection 3.4 is devoted to the study of the energetics of several local polar configurations embedded in the PE phase in both compounds. In Subsections 3.5 and 3.6 we present a thorough study of quantum fluctuations, and the controversial problem of the isotope effects. In particular, in Subsection 3.5 we analyze the geometrical effects and the issue of tunneling at fixed potential and discuss important consequences for these compounds. We also provide in Subsection 3.6 an explanation for the giant isotope effect observed in KDP by means of a self-consistent quantum mechanical model based on the ab initio data. Similar implications for ADP and other compounds of the H-bonded ferroelectrics family are also discussed. In Subsection 3.7 we review additional ab initio results obtained for KDP: pressure effects, structure and energetics of Slater and Takagi defects and the development of an atomistic model. Finally, in Section 4 we discuss the above issues and present our conclusions.

2. *Ab initio* method and computational details

The first-principles calculations have been carried out within the framework of the density functional theory (DFT), (49; 50) using the SIESTA program. (51; 52) This is a fully self-consistent DFT method that employs a linear combination of pseudoatomic orbitals (LCAO) of the Sankey-Niklewsky type as basis functions (53). These orbitals are strictly confined in real space, what is achieved by imposing the boundary condition that they vanish at a certain cutoff radius in the pseudoatomic problem (i.e. the atomic problem where the Coulomb potential was replaced by the same pseudopotential that will be used in the solid state). With this confinement condition, the solutions are slightly different from the free atom case and have somewhat higher energy. In this approximation, the relevant parameter is precisely the orbital confinement energy E_c which is defined as the difference in energy between the eigenvalues of the confined and the free orbitals. We set in our calculations a value of E_c=50 meV. By decreasing this value further we have checked that we obtain total energies and geometries with sufficient accuracy. In the representation of the valence electrons, we used double-zeta bases with polarization functions (DZP), i.e. two sets of orbitals for the angular momenta occupied in the isolated atom, and one set more for the first nonoccupied angular momentum (polarization orbitals). With this choice, we again obtain enough accuracy in our calculations.(47; 48)

The interaction between ionic cores and valence electrons is represented by nonlocal, norm-conserving pseudopotentials of the Troullier-Martins type.(54) The exchange-correlation energy functional was computed using the gradient-corrected Perdew-Burke-Ernzerhof (PBE) approximation.(55) This functional gives excellent results for the equilibrium volume and bulk modulus of H-bonded ice Ih when compared to other approximations.(56) On the other hand, the BLYP functional,(57; 58) which gives very good results for molecular H-bonded systems,(59) yields results of quality inferior to PBE when used in the solid state.(48) The real-space grid used to compute the Coulomb and exchange-correlation numerical integrals corresponded to an equivalent energy cutoff of 125 Ry. These approximations, especially those related to the confinement of the pseudoatomic orbitals, were also tested against results from standard pseudopotential plane-wave calculations. (48)

The PE phases of KDP and ADP have a body-centered tetragonal (*bct*) structure with 2 formula units (f.u.) per lattice site (16 atoms in KDP and 24 atoms in ADP). For the calculations

that describe homogeneous distortions in KDP, we used the conventional *bct* cell (4 f.u.), but doubled along the tetragonal *c* axis. This supercell comprises 8 f.u. (64 atoms). A larger supercell is required to describe local distortions. To this end, we used the equivalent conventional fct cell (containing 8 f.u., and axes rotated through 45 degrees with respect to the conventional *bct* cell), also doubled along the *c*-axis (128 atoms). For the different phases studied for ADP (FE, AFE, PE), we used the equivalent conventional fct cell. In the following, and unless we state the contrary, the calculations were conducted using a Γ-point sampling of the Brillouin zone (BZ), which proved to be a good approximation due to the large supercells used.(48) The calculations of local distortions in ADP were performed in a 16 f.u. supercell using a 6 k-points BZ sampling, which proved sufficient for convergence.(60)

3. *Ab initio* results

3.1 Characterization of the structures of KDP and ADP

We have performed different computational experiments with the aim of characterizing all phases of KDP and ADP. First, we optimized the PE phase structure of KDP. To this end, we fixed the lattice parameters to the experimental values at T_c+5 K in the conventional *bct* cell,(61) and constrained the H-atoms to remain centered in the O-H$\cdots$O bonds. The full-atom relaxation in these conditions leads to what we call the centered tetragonal (CT) structure, which can be interpreted as an average structure (H_O's centered in the H-bonds) of the true PE phase.(48) Actually, neutron diffraction experiments have shown that the hydrogens in this phase occupy with equal probability two equivalent positions along the H-bond distant $\delta/2$ from the center (Fig. 2).(4; 62) The results of the relaxations with the above constraint for the H to maintain the PE phase show a satisfactory agreement of the structural parameters compared to the experiment, except for the d_{OO} distance which turns out to be too short (see Table 1).

We also relaxed all the internal degrees of freedom, but now fixing the simulation cell to the experimental orthorhombic structure at $T_c - 10\ K$ in the conventional fct cell. (61) The calculated geometrical parameters are shown in Table 1 compared to experimental data. In general the agreement is quite reasonable, again with the exception of the O-O distance.

A detailed analysis revealed that the underestimation in the O-O bond length originates from the approximate character of the exchange-correlation functional, although in the case of the PE phase, it is due in part to the constraint imposed.(48) In fact, it is found in GGA gas-phase calculations of $H_3O_2^-$ an underestimation in d_{OO} of $\approx$ 0.06 Å when compared to quantum chemical calculations.(63) Moreover, first-principles test calculations indicate a similar underestimation for the water dimer O-O distance compared to the experimental values.(48; 64) On the other hand, the potential for protons or deuterons in the H-bond is very sensitive to the O-O distance.(48) Thus, in order to avoid effects derived from this feature in the following calculations, the O-O distances are fixed to the experimental values observed in the PE phase, unless we state the contrary.

Using a similar procedure, we calculated the PE structure of ADP.(60) We found that the agreement is good compared to the experimental data, as is shown in Table 1.(65; 66) In a second step, we relaxed all atom positions but now fixing the lattice parameters to the orthorhombic experimental cell of ADP.(65) In this case, we have also allowed the O-O distance to relax, since we were interested in the overall structure. The relaxation in the orthorhombic structure leads to an AFE phase in fair agreement with the experiment (see

Table 1). Although the calculated P-O bonds are somewhat longer than the experimental values, the degree of tetrahedra distortion measured by the difference between d(P-O_2) and d(P-O_1) is well reproduced by the calculations. The calculated O-O distance is now underestimated only by 1.5% in comparison to the experimental value, which is again due to the approximation of the exchange-correlation functional as explained above. Although the N-H$\cdots$O distance is in general well reproduced, the calculated geometry of NH_4^+ turns out to be a little expanded respect to the experiment. This could be ascribed to an underestimation in the degree of covalency of the N-H bond due to the orbital-confinement approximation in the first principles calculation with the SIESTA code. On the other hand, the proton shift $\delta/2$ from the H-bond center turns out to be about half the value of that from the x-ray experiment (see Table 1). However, high resolution neutron diffraction results of δ for ADP lie close to the corresponding value for the isomorphic compound KDP,(62) which is ≈ 0.34 Å at atmospheric pressure, in fair agreement with the present calculations. Moreover, our calculated value of δ is close to that found in ab initio calculations for KDP, (48) which is reasonable since the H-bond geometry is expected to depend mostly on the local environment which is similar for both compounds. Therefore, we conclude that the experimental value of δ in the AFE phase of ADP, as is shown in Table 1, may be overestimated because of the low resolution of x-rays to determine proton positions.(65)

In the calculated AFE structure arising from the all-atom relaxation (see the schematic plot for the pattern of atom distortions in Fig. 3 (c)), the ammonium ion displaces laterally about $u_N^{min} = 0.09$ Å producing a dipole that reinforces that determined by the lateral arrangement of acid protons in the phosphate. On the other hand, if we allow the system to relax following the FE pattern in ADP as shown in Fig. 3(b), the relaxed structure is that plotted schematically in Fig. 1 (b) with an energy slightly higher than that for the AFE minimum. (21) In this calculated FE phase of ADP, the ammonium ion displaces along z about 0.05 Å reinforcing the z dipoles produced by the arrangement of acid protons in the phosphates, which is analogous to the behavior of the K^+ ion in KDP (see FE mode in KDP as plotted in Fig. 2). (47; 48)

3.2 Charge redistributions associated with the instabilities in KDP and ADP

We have analyzed the charge redistributions produced by the ordered proton off-centering in KDP (48) and ADP (60). To this aim, we computed the changes in the Mulliken orbital and bond-overlap populations in going from the PE phases to the FE and AFE phases of KDP and ADP, respectively. We have also performed the analysis of the charge redistributions in the non-observed FE phase of ADP. The ordered phases for both compounds were calculated in a hypothetical tetragonal structure in order to be able to compute charge differences related to the PE phase. (46; 48) Mulliken populations depend strongly on the choice of the basis set. Differences, however, are much less sensitive. The results are shown in Table 2 for the atoms and bonds pertaining to the O-H$\cdots$O bridges and the phosphates in both materials (also shown is the K atom population for KDP).

As a common feature for both compounds, we observe an increase of the charge localized around O_1 with the main contribution provided by a decrease in the O_2 charge. This is followed by an increase in the acid hydrogen population for ADP and minor charge redistributions in the remaining atoms for both compounds. The significant enhancement of the population of the O_1 atom is also accompanied by an increase in the bond overlap population of the O_2-H, and O_1-P bonds and a decrease of this magnitude in the $O_1 \cdots$H and O_2-P bonds. The trends observed in Table 2 are confirmed by charge density difference plots

Structural parameters	PE				AFE(ADP)		FE(KDP)	
	ADP		KDP					
	AI	Exp	AI	Exp[c]	AI	Exp[a]	AI	Exp[c]
a	-	7.473 [a]	-	7.426	-	7.503	-	10.546
b	-	7.473 [a]	-	7.426	-	7.512	-	10.466
c	-	7.542 [a]	-	6.931	-	7.488	-	6.926
d(O-O)	-	2.481 [a]	2.407	2.483	2.462	2.50	2.446	2.497
$d(O_2\text{-}H_O)$	1.240	1.049 [b]	1.204	1.071	1.093	0.90	1.108	1.056
δ	0	0.377 [b]	0	0.341	0.277	0.70	0.230	0.385
$d(P\text{-}O_1)$	1.541	1.538 [b]	1.592	1.543	1.572	1.522	1.572	1.516
$d(P\text{-}O_2)$	1.541	1.538 [b]	1.592	1.543	1.618	1.566	1.618	1.579
$<O_1\text{-}P\text{-}O_1$	108.6	108.6 [b]	108.6	110.6	111.7	112.5	114.5	114.6
$<O_2\text{-}P\text{-}O_2$	108.6	108.6 [b]	108.6	110.6	104.6	104.7	107.6	106.7
$<O_1 \cdots H\text{-}O_2$	180.0	177.1 [b]	176.6	178.2	175.3	-	176.8	179.4
$d(N\text{-}H^1_N)$	1.048	1.002 [b]	-	-	1.052	0.90	-	-
$d(N\text{-}H^2_N)$	1.048	1.002 [b]	-	-	1.042	0.83	-	-
$d(N\text{-}O_1)$	3.170	3.172 [b]	-	-	3.139	3.152	-	-
$d(N\text{-}O_2)$	3.170	3.172 [b]	-	-	3.182	3.152	-	-
$d(N\text{-}H^1_N ... O_1)$	2.895	-	-	-	2.779	-	-	-
$d(N\text{-}H^2_N ... O_2)$	2.895	-	-	-	2.923	-	-	-

Table 1. Comparison of the *ab initio* (AI) calculated internal structure parameters of KDP and ADP (Ref.(60)) with experimental data for the PE, AFE(ADP) and FE(KDP) phases considered in the text. Distances in Å and angles in degrees.
[a] Ref. (65); [b] Ref. (66); [c] Ref. (61)

in these systems. (21; 46; 48) Thus, when the protons displace off-center and approach the O_2 atom, the charge localizes mostly in the O_1 atom and to a lesser extent in the O_1-P orbitals. This is accompanied by a weakening of the $O_1 \cdots H$ bond and a strengthening of the O_1-P bond, which shortens (see Table 1). On the other hand, the charge flows away from the O_2 atom and the O_2-P bond and localizes mostly in the O_2-H bond which strengthens. Then, the PO_4 tetrahedron distortion as observed in Table 1 is a consequence of the strengthening and weakening of the O_1-P and O_2-P bonds respectively, as the protons displace off-center in the H-bonds. The overall effect of the acid H's off-centering in the PO_4 + acid H-bond subsystem of ADP and KDP can be summarized as a flow of electronic charge from the O_2 side of the phosphate tetrahedron towards the O_1 side with a concomitant modification of its internal geometry. Thus, the charge redistributions results for the acid H-bonds shown in Table 2 enable us to conclude that the behavior for these bonds in both compounds are very similar. (21; 46; 48) A schematic view of the displacements of the atoms along the FE mode in KDP and the accompanying electronic charge redistributions produced upon off-centering of the H-atoms is shown in Fig. 2.

We have also compared in ADP the behavior of the N-H$\cdots$O bonds between oxygen and ammonium in the AFE phase with that in the hypothetical FE one (See the schematic lateral view in Fig. 3(b)).(60) To this aim, we computed the changes in the Mulliken orbital and bond-overlap populations for these bonds in going from the PE to the AFE and FE configurations. The results are shown in Table 3. When the acid H's are displaced with the FE pattern of Fig. 3 (b), all H_N's remain equivalent and the O$\cdots$$H_N$ bonds weaken. This

Phase	O_1	O_2	P	H	O_1-P	O_2-P	$O_1 \cdots$ H	O_2-H	K
FE(KDP)	+82	-58	-8	-17	+46	-44	-91	+70	-3
AFE(ADP)	+100	-151	+5	+35	+44	-33	-98	+91	-
FE(ADP)	+93	-151	+2	+36	+52	-43	-91	+86	-

Table 2. Changes $\Delta q = q(x) - q(PE)$ (x = AFE,FE for ADP or FE for KDP) in the Mulliken orbital and bond overlap populations in going from the PE to the AFE and FE phases in ADP (60) or to the FE phase in KDP (48). Shown are populations of the atoms and bonds belonging to the phosphates and the O-H$\cdots$O bridges in both compounds. Also reported is the result for the K atom in KDP. Units in e/1000.

Phase	N	H^2_N	H^1_N	N-H^1_N	N-H^2_N	$O_1 \cdots H^1_N$	$O_2 \cdots H^2_N$
AFE	+7	+7	-9	-4	+4	+16	-14
FE	+1	+1	+1	+3	+3	-7	-7

Table 3. Changes $\Delta q = q(x) - q(PE)$ (x = AFE or FE) in the Mulliken orbital and bond overlap populations in going from the PE to the AFE and FE phases in ADP (60). Shown are populations of the atoms and bonds belonging to the NH_4^+ ions and the N-H$\cdots$O bridges . Units in e/1000.

behavior is compatible with the decrease in the bond overlap population for this bond in Table 3. On the contrary, with the AFE distortion (see Fig. 3(c)), the arising short and long N-H$\cdots$O bonds behave in an opposite way. In fact, the long N-$H^2_N \cdots O_2$ bond suffers a decrease in the $O_2 \cdots H^2_N$ bond overlap population and a weakening of the bond while the corresponding magnitude of the short N-$H^1_N \cdots O_1$ bond increases and the bond strengthens. The charge variations are observed to be nearly twice the corresponding value for the analogue magnitude in the FE phase. Similarly, in the AFE phase the N-H^2_N bond strengthens with a slight increment in the bond overlap population and the N-H^1_N bond weakens with a decrease in the localized charge. These charge redistributions in the ammonium tetrahedron give rise to its distortion (see Table 1). As a consequence, we observe a charge flow from the long to the short N-H$\cdots$O bonds which is concomitant to the ammonium distortion, absent in the FE phase.(60) This behavior is also observed in charge density difference plots for ADP.(21) In the next Section we discuss how the charge flow inside ammonium and its distortion are related to the stabilization of the AFE phase over the FE one in ADP.(21)

3.3 Origin of antiferroelectricity in ADP

With the aim of studying the AFE and FE instabilities and their relative importance in ADP, we have performed different calculations.(21) First we consider the joint displacement of N and acid H_O protons from their centered positions in the PE phase, denoted by u_N and u_{H_O} respectively. These are performed in two cases: (i) following the AFE pattern of distortion (see Fig. 3(c)), and (ii) following the FE pattern (see Fig. 3(b)). The H_N's of the ammonium and P's are allowed to relax (this is always the case unless we state the contrary), while the O's remain fixed for the reasons explained in Subsection 3.1. The ab-initio total-energy curve is plotted in Fig. 3(a) as a function of u_{H_O}, for the concerted motion of H_O and N corresponding to each pattern. We observe that the calculated minimum-energy AFE state is only slightly more stable than the FE counterpart, with a small energy difference of 3.6 meV/f.u. (f.u. = formula unit). With the O's relaxations the AFE state remains 1.25 meV/f.u. below the FE one. If we additionally relax the lattice parameters according to the symmetries of each phase, this difference grows to $\approx$ 3.8 meV/f.u. We have also determined recently the closeness in energy to the AFE state of two other possible ordered phases with translational symmetry and xy-polarized PO_4 tetrahedra.(21) Thus, we confirm the closeness between the AFE and FE

states in ADP, a fact that suports Ishibashi's model (19; 20) and also provides an explanation for the coexistence of AFE and FE microregions near the AFE transition.(25; 26)

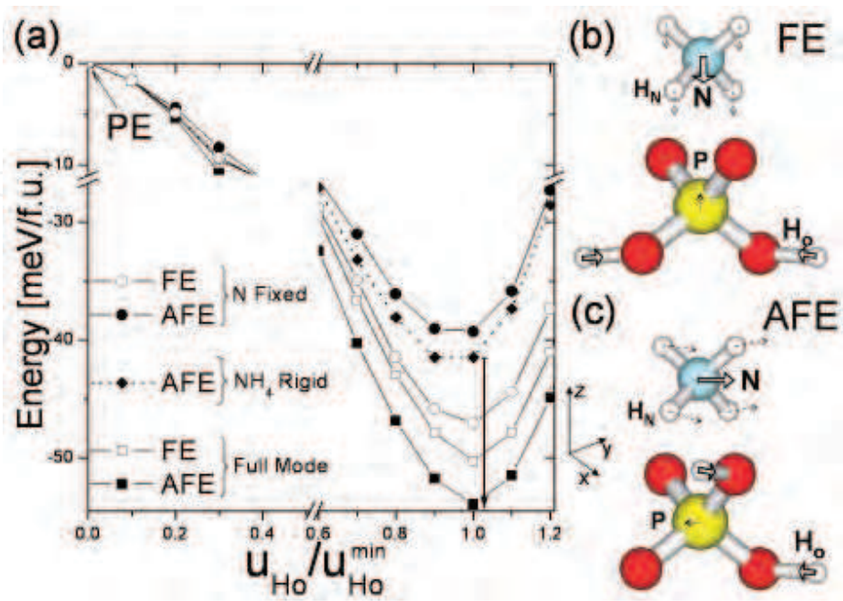

Fig. 3. (a) Energy as a function of the acid H displacement u_{H_O} for different patterns of atomic displacements corresponding to the FE and AFE distortions depicted in Figs. 3(b) and 3(c) respectively. $u_{H_O}^{min}$ denotes the H_O displacement at the corresponding energy minimum. In addition to the full FE or AFE modes, other curves show the effect of imposing different constraints while performing the FE or AFE modes: N fixed or NH_4^+ moved rigid as in the PE phase. Lateral views of the ADP formula unit indicate the atomic displacements in the (b) FE and (c) AFE modes. White arrows correspond to displacements imposed according to each mode, dashed arrows to accompanying relaxations.

In order to determine the mechanism for the stabilization of the AFE vs FE state, we also considered the energy contribution of the N and H_O motion separately.(21) If we set $u_{H_O} = 0$, a finite displacement u_N along z (see Fig. 3(b)) does not contribute to any energy instability in the FE case. Moreover, the N displacement along the xy-plane in the AFE case (see Fig. 3(c)) produces a very tiny instability (less than 1 meV/f.u.). Alternatively, we move the acid H_O's and set $u_N = 0$, i.e. N's are fixed to their positions in the PE phase (see Figs. 3(b) and 3(c)). We observe in this case a larger energy decrease for the FE pattern compared to the AFE one (see circles in Fig. 3(a)). It is worth mentioning that here the H_N's relaxations in the ammonium are very small in contrast with the case where both N and H_O's are allowed to displace. In the FE case, a further energy decrease of less than 10% of the total instability is achieved when the N's are allowed to move together with the H_O's (see open circles and squares at the energy minima in Fig. 3(a)). The fact that the FE-pattern relaxation with $u_{H_O} = 0$ does not produce any instability prompts us to conclude that the source of the FE instability in ADP is the acid proton off-centering ($u_{H_O} \neq 0$), similar to what is found in KDP.(48) The proton off-centering also produces the AFE instability, but this motion alone is insufficient to explain antiferroelectricity in ADP.(21)
Finally, we have considered the displacements of all atoms following the pattern of the AFE mode, with the only constraint that the structure of the NH_4^+ groups is kept rigidly symmetric

as in the PE phase.(21) The energies obtained in this case are shown by solid diamonds in Fig. 3(a), which have to be compared to those corresponding to the full relaxation of the FE phase by open squares (in the last case H_N relaxations in the NH_4^+ groups are negligible). We observe that the FE state is more stable than the AFE one as long as the NH_4^+ tetrahedra are not allowed to deform by relaxing their H_N's. Notice that by not allowing the relaxation of the ammonium, this ion behaves in the same way as the K^+ ion in KDP, where the FE phase is more stable than the AFE distortions.(48; 67) If we allow for the optimization of the N-H$\cdots$O bridges by relaxing the NH_4^+, the stabilization of the AFE state against the FE one is achieved. This energy decrease is visualized in Fig. 3(a) by the arrow between full diamonds and squares at $u_{H_O}/u_{H_O}^{min} = 1$. Therefore, the origin of antiferroelectricity in ADP is ascribed to the optimal formation of N-H$\cdots$O bridges.(21) This conclusion is further supported by a study of the energy variation produced by a global rigid rotation of the NH_4^+ molecules around the z-axis.(21)

3.4 Local instabilities and the nature of the PE phases of KDP and ADP

The observed proton double-occupancy in the PE phases of KDP and ADP,(38; 61; 62) is an indication of the order-disorder character of the observed transitions. The origin of this phenomenon can be ascribed either to static or thermally activated dynamic disorder, or to tunneling between the two sites. The physics behind these scenarios is intimately connected to the instabilities of the system with respect to correlated but localized H motions in the PE phase, including also the possibility of heavy-ions relaxation.

We have analyzed localized distortions by considering increasingly larger clusters embedded in a host PE matrix of KDP (47; 48) and ADP (60). For the reasons exposed above, the host is modeled by protons centered between oxygens, and the experimental structural parameters (including the O-O distances) of KDP and ADP in their PE phases.(61; 65) In order to assess the effect of the volume increase observed upon deuteration, we also analyzed the analogous case of D in DKDP by expanding the host structural parameters to the corresponding experimental values.(47; 48; 61) We also compared qualitatively the effect of volume expansion in ADP by considering a larger equilibrium O-O distance in the lattice.(60) The trends are compared qualitatively to the case of KDP, although we have to bear in mind that the instabilites in both systems have a different character (FE in KDP and AFE in ADP).

First, we considered distortions for clusters comprising N hydrogens (deuteriums) in KDP: (a) N=1 H(D) atom, (b) N=4 H(D) atoms which connect a PO_4 group to the host, (c) N=7 H(D) atoms localized around two PO_4 groups, and (d) N=10 H(D) atoms localized around three PO_4 groups. The correlated motions follow the pattern for the FE mode shown in Fig. 2.

We represented the correlated pattern with a single collective coordinate x whose value coincides with the H(D) off-center displacement $\delta/2$ (see Fig. 2). Notice that this coordinate is equivalent to that defined above as u_{H_O} for the proton off-centering. For the sake of simplicity, we considered equal displacements along the direction of the O-O bonds for all the hydrogen atoms in the cluster. Two cases were considered: (i) first, we imposed displacements only on H atoms, maintaining all other atoms fixed, (ii) second, we also allowed for the relaxation of the heavy ions K and P, which follow the ferroelectric mode pattern as expected (Fig. 2). In a next step, we quantized the cluster motion in the corresponding effective potential to determine the importance of tunneling in the disordered phase of KDP. Although, rigorously speaking, the size dependence should be studied for larger clusters than those mentioned here, short-range

quantum fluctuations in the PE phase are sufficiently revealing, especially far away from the critical point.

We show in Fig. 4(a) and Fig. 4(b) the total *ab initio* energy as a function of the collective coordinate x for the clusters considered in KDP and DKDP, respectively.(47; 48) In the case of KDP, all the clusters considered are stable if only hydrogens are displaced. Actually, the largest cluster calculated (N=10) is very stable, as indicated by the open circles in Fig. 4(a). In the expanded lattice of DKDP, results indicate a small barrier of $\sim$ 6 meV for the N=7 move, and a larger value of $\approx$ 25 meV for the N=10 cluster (see open squares and circles respectively in Fig. 4(b)).

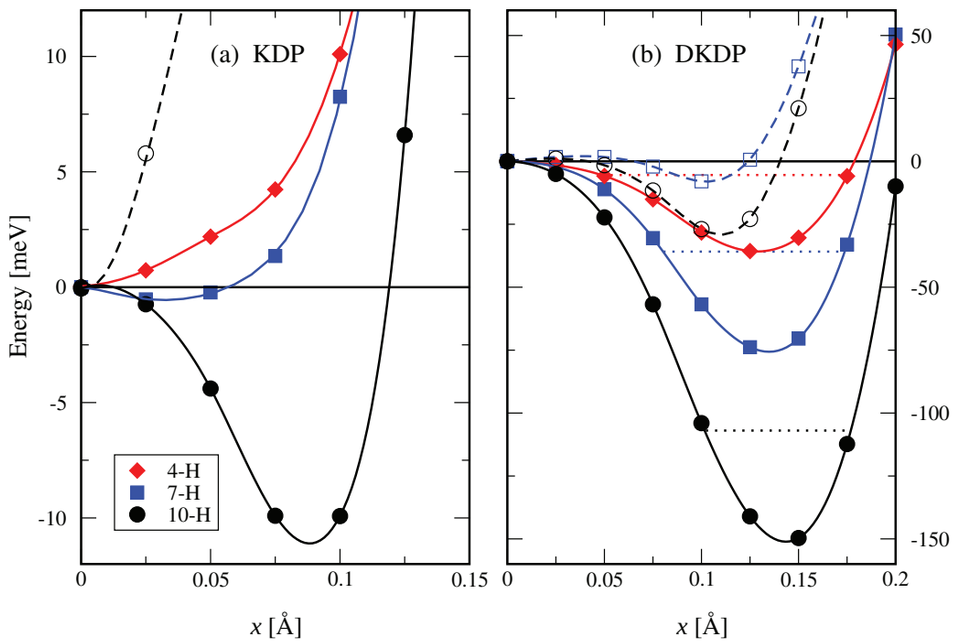

Fig. 4. Energy profiles for correlated local distortions in (a) KDP and (b) DKDP. Reported are clusters of: 4 H(D) (diamonds), 7 H(D) (squares), and 10 H(D) (circles). Empty symbols and dashed lines indicate that only the H(D) atoms move. Motions that involve also heavy atoms (P and K) are represented by filled symbols and solid lines. Negative GS energies signaling tunneling, are shown by dotted lines. Lines are guide to the eye only.

The energy profiles vary drastically when we allow the heavy atoms relaxations for the above correlated motions in KDP.(47; 48) Now, clusters involving two or more PO_4 units exhibit instabilities in both KDP and DKDP. In the case of the N=10 cluster, the barrier in DKDP is of the order of 150 meV. The appearance of these instabilities provides a measure of the FE correlation length in the system. In the expanded DKDP lattice, the instabilities are much stronger, and the correlation length is accordingly shorter than in KDP.

In the next step, we solved the Schrödinger equation for the collective coordinate x for each cluster in the corresponding effective potentials of Fig. 4.(47; 48) To this aim, we calculated the effective mass for the local collective motion of the cluster as $\mu = \sum_i m_i a_i^2$, where i runs over

the displacing atoms and m_i are their corresponding atomic masses. In this equation, a_i is the i-atom displacement at the minimum from its position in the PE phase, relative to the H(D) displacement.

In the cases where only the N deuteriums are displaced in the unstable clusters of DKDP (see Fig. 4(b)), all by the same amount, the calculated ground states (GS) energies lie above the barriers. Thus, tunneling of H (D) alone seems to be precluded as an explanation of the double site occupancy observed in the PE phases of KDP and DKDP, at least for clusters of up to 10 hydrogens (deuteriums).(47; 48)

When the heavier atoms are allowed to relax, the effective masses per H(D) calculated for these correlated motions in different clusters are about $\mu_H \approx 2.3$ ($\mu_D \approx 3.0$) proton masses (m_p) in KDP (DKDP), respectively. The resulting GS energy levels are quantized below the barrier for all clusters including the heavy atoms motion in DKDP (see dotted lines in Fig. 4(b)). Thus, there is a clear sign of tunneling for the correlated D motions involving also the heavy ions.(47; 48) These collective motions can be understood as a local distortion reminiscent of the global FE mode. (68) On the other hand, even the largest cluster considered (N=10) in KDP, has the GS level quantized above the barrier. The critical cluster size where the onset of tunneling is observed provides a rough indication of the correlation volume: it comprises more than 10 hydrogens in KDP, but no more than 4 deuteriums in DKDP. Thus, the dynamics of the order-disorder transition would involve fairly large H(D)-clusters together with heavy-atom (P and K) displacements. The observed proton double-occupancy is explained in our calculations by the tunneling of large and *heavy* clusters.(47; 48) This is confirmed by the double-site distribution determined experimentally for the P atoms. (69; 70)

In the case of ADP, we have analyzed local cluster distortions embedded in its PE phase.(60) We considered the experimental lattice in this phase,(65) and in order to vary the O-O distance, the PO_4 tetrahedra were rotated rigidly. We also let the ammonium relax to optimize the N-H$\cdots$O bridges. We considered displacements of N=1 proton, and also clusters of N=4 and N=7 simultaneously displaced acid protons from their centered positions in the H-bonds while keeping fixed the rest of the atoms. In the cases of N=4 and N=7 protons the displacement patterns correspond to the AFE mode (see Fig. 1(a) and Fig. 3(c)). We calculated the total energy for each configuration. We plot in Fig. 5 the resulting potential profiles for the protons along the bridges as a function of their off-center displacements u_{H_O} from the middle of the H-bonds. We observe that the off-centering of a single proton leads to an energy minimum, at variance with the case of KDP.(48; 67) This behavior in ADP has to be ascribed to the energy contributions of N-H$\cdots$O bridges, which compensate the energy increase due to the formation of Takagi pair defects. The variation of the O-O distance does not affect this energy minimum, as well as the one observed at lower displacements for the N=4 and N=7 proton movements, thus confirming that it can be related to the N-H$\cdots$O bridges in the three cases.(60) On the other hand, we observe that the second minimum at larger distances is strongly dependent on the O-O distance. In fact, this minimum is incipient at d_{OO}=2.48 Å and is clearly seen at d_{OO}=2.52 Å for the N=4 and N=7 proton displacements. This instability is therefore ascribed to favorable lateral Slater configurations related to the O-H$\cdots$O bonds.(17; 60) The same bonds favor the formation of local polar configurations in KDP at a similar H off-centering distance $\delta/2$ (see Fig. 4).(47; 48) This minimum becomes deeper for larger proton clusters and is located at a H off-centering distance which approaches the one corresponding to the global ordered phases in both compounds.(21; 47)

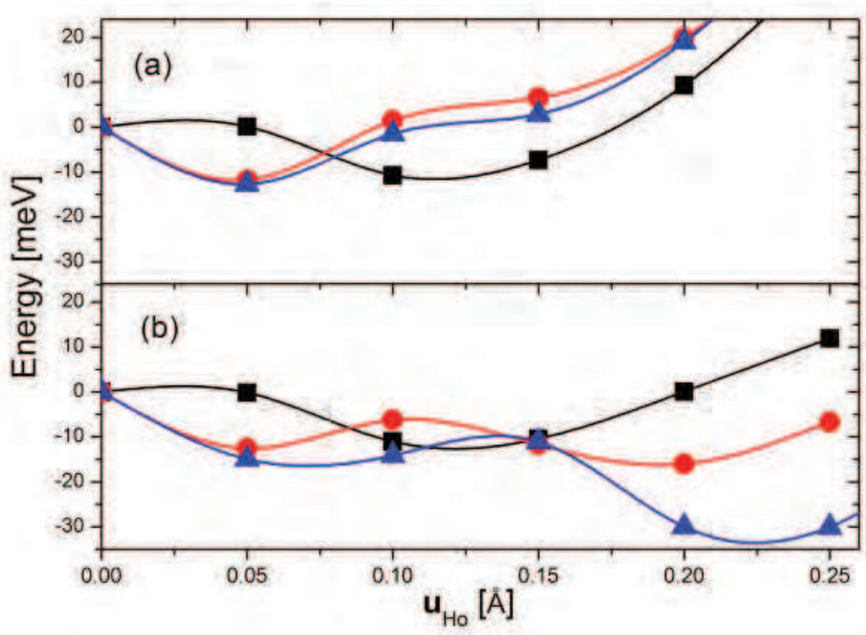

Fig. 5. Energy profiles for correlated proton distortions along the acid H-bonds as a function of the acid proton displacement u_{H_O} in ADP. The results are shown for different O-O distances in the crystal: a) d_{OO}=2.48 Å and b) d_{OO}=2.52 Å. Reported are clusters of N=1 H (squares), N=4 H (circles), and N=7 H (triangles).

3.5 Geometrical effect vs tunneling

Let us now address the origin of the huge isotope effect on T_c, observed in KDP and its family. After the pioneering work of Blinc,(27) the central issue in KDP has been whether tunneling is or is not at the root of the large isotope effect. However, this fact was never rigorously confirmed, in spite of the large efforts made in this direction. Recently, a crucial set of experiments done by Nelmes and coworkers indicated that the tunneling picture, at least in its crude version, does not apply. Actually, by applying pressure and tuning conveniently the D-shift parameter δ, they brought T_c^{DKDP} almost in coincidence with T_c^{KDP}, in spite of the mass difference between D and H in both systems. (4; 38; 62) This indicates that the modification of the H-bond geometry by deuteration – the *geometrical effect* – is the preponderant mechanism that accounts for the isotope effects in the transition.

The tunnel splitting Ω tends to vanish as the cluster size grows ($N \to \infty$).(47; 48) On the other hand, it is expected that for the nearly second-order FE transition in these systems,(71) only the large clusters are relevant. For large tunneling clusters, the potential barriers are large enough and the GS levels are sufficiently deep (see Fig. 4) that the relation $\hbar\Omega_{H(D)} \ll K_B T_c$ is fulfilled so much for D as for H. The above relation implies, according to the tunneling model, that a simple change of mass upon deuteration at fixed potential could not explain the near doubling of T_c. Let us consider the largest cluster (N=10) in Fig. 4 for DKDP, which is larger than the crossover length in this system. In this case, the GS level amounts to E_{GS} = -107 meV (calculated with a total effective mass of $\mu_D = 35.4\ m_p$). This value is well below the central barrier. The corresponding tunneling splitting is of the order of $\hbar\Omega_D = 0.34$ K. If we maintain

the potential fixed, and change the cluster effective mass to that for the non-deuterated case ($\mu_H = 25.3\ m_p$), the calculated tunnel splitting is now only slightly larger $\hbar\Omega_H = 1.74$ K. As $T_c^{DKDP} \approx 229K$, the relation $\hbar\Omega_{H(D)} \ll K_B T_c$ is clearly satisfied. As a consequence, a small change in T_c should be expected by the sole change of Ω at fixed potential. This conclusion agrees with the neutron diffraction results at high pressure,(4; 38; 62) where the isotope effect in T_c appears to be very small at fixed structural conditions.

We plot in Fig. 6 (a) the calculated proton and deuteron wave functions (WF) in the DKDP fixed potential for the N=7 cluster. The plot shows very slight differences between both WF. Moreover, the distance between peaks as a function of the effective mass at fixed potential remains almost unchanged, as can be seen by the square symbols in Fig. 6 (c). We conclude that the geometric effect in the H-bond at fixed potential is very small.(47; 48)

In constrast to the case of DKDP, the proton WF for the N=7 cluster in the KDP potential exhibits a broad single peak, as shown in Fig. 6 (a). Now, this question emerges: How can we explain such a big geometric change in going from DKDP to KDP? After this question, the first observation comes from what is apparent in Fig. 4: energy barriers in DKDP are much larger than those in KDP, implying that quantum effects are significantly reduced in the expanded DKDP lattice. On the other hand, we observe in Fig. 6(a) that the proton WF in KDP has more weight around the middle of the H-bond ($\delta_c \approx 0$, where δ_c is the collective coordinate) than in DKDP. In other words, due to quantum delocalization effects the proton is more likely to be found at the H-centered position between oxygens than the deuteron. Consequently, as the proton is pushed to the H-bond center due to zero-point motion the covalency of the bond becomes stronger. The mixed effect of quantum delocalization and gain in covalency leads to a geometric change of the O-H$\cdots$O bridge, which in turn affects the crystal cohesion. In fact, the increased probability of the proton to be midway between oxygens, strengthens the O-H$\cdots$O covalent grip and pulls the oxygens together, causing a small shrinking of the lattice. The effect of this shrinking is to decrease the potential depth, making the proton even more delocalized. This produces again an increase in the covalency of the O-H$\cdots$O bond, pulling effectively the oxygens together, an so on in a self-consistent way. We have identified this self-consistent phenomenon as the one that shrinks the lattice from the larger classical value to the smaller value found for KDP.(47; 48) Thus, the large geometrical effect in these systems is attained by this self-consistent phenomenon, which in turn is triggered by tunneling. The overall effect is eventually much larger than the deuteration effect obtained at fixed potential. The upper limit to the effect described above was evaluated with additional classical electronic calculations by looking at the effects of H-centering in the FE phase of KDP.(47; 48) It was found that the lattice volume shrinks about 2.3 % upon centering the H's. Moreover, at the equilibrium volume, the proton centering creates an equivalent pressure of $\approx$ 20 kbar. However, the protons are equally distributed on both sides of the bond in the true high-temperature PE phase, thus reducing the magnitude of the effect.

3.6 The nonlinear self-consistent phenomenon and the isotope effects

The large geometric effect observed due to deuteration may be explained, as discussed in the previous subsection, by a self-consistent mechanism combining quantum delocalization, the modification of the covalency in the bond, and the effect over the lattice parameters. The mechanism is also capable of explaining, at least qualitatively, the increase in the order parameter and T_c with deuteration. The origin of the self-consistent phenomenon is the

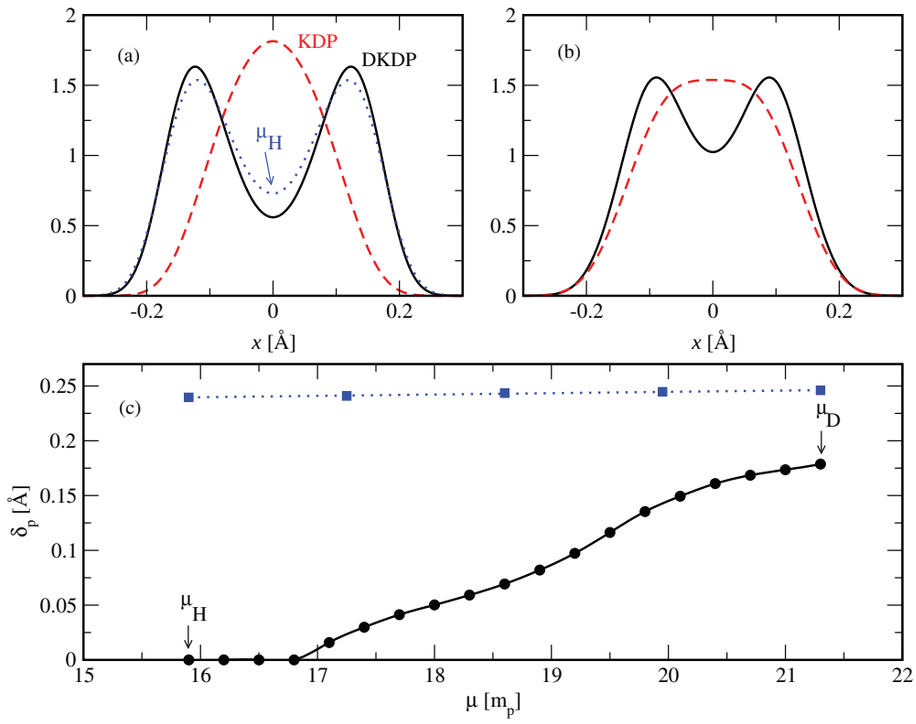

Fig. 6. WF for the 7-H(D) cluster potential for (a) *ab initio* and (b) self-consistent model calculations. Solid (dashed) lines are for D (H). Dotted line is for H in the DKDP potential. (c) WF peak separation δ_p as a function of the cluster effective mass μ (given in units of the proton mass) for the self-consistent model (circles) and for fixed DKDP potential (squares). Lines are guides to the eye.

difference in tunneling induced by different masses, but is strongly amplified through the geometric modification of the lengths and energy scales.

We have constructed a simple model which accounts for the non-linear self-consistent behavior described above.(47; 48) To this aim, we considered the Schrödinger equation for the clusters by adding to the underlying hydrogen potential a quadratic WF-dependent term. The effective potential now reads:

$$V_{\text{eff}}(x) = V_0(x) - k|\Psi(x)|^2, \tag{1}$$

where $x = \delta_c/2$ and $V_0(x)$ is a quartic double-well similar to those of Fig. 4. The quadratic term $|\Psi(x)|^2$ produces the non-linear feedback in the model. In fact, the enhancement of the proton delocalization relative to the deuteron leads to an increase of $|\Psi(x)|^2$ at the center (increased probability to be found at the middle of the H-bond), which in turn produces a decrease in the barrier for the effective potential, which further delocalizes the proton, and so on until self-consistency is achieved. The bare potential is written as follows:

$$V_0(x) = E_b^0 \left[-2 \left(\frac{2x}{\delta_{min}^0} \right)^2 + \left(\frac{2x}{\delta_{min}^0} \right)^4 \right], \tag{2}$$

in terms of its energy barrier E_b^0 and minima separation δ_{min}^0. We have chosen the parameters values k = 20.2 meV Å, E_b^0 = 35 meV and δ_{min}^0 = 0.24 Å to qualitatively reproduce the WF profiles in the cases of KDP (broad single peak) and DKDP (double peak), for the same cluster size.(47; 48) The WF self-consistent solutions depend only on the effective mass μ, once these parameters are fixed. We show in Fig. 6 (b) the WF corresponding to μ_D (solid line) and μ_H (dashed line), which are similar to those calculated from the ab initio potentials for the N=7 cluster (Fig. 6 (a)). Also shown in Fig. 6 (c) is the distance between peaks δ_p in the WF as a function of μ. Starting from the finite value for μ_D (DKDP), Fig. 6 (c) shows how δ_p decreases remarkably towards lower μ values for the self-consistent solution. This happens until it vanishes near μ_H (KDP) (see circles in Fig. 6(c)). This behavior is in striking contrast with the very weak dependence obtained at fixed DKDP potential and geometry (square symbols in Fig. 6(c)). The amplification in the self-consistent geometrical modification of the H-bond, as is evidenced by the large mass dependence of the WF in Fig. 6(c), can now explain satisfactorily the large isotope effect found in KDP.(47; 48)

We have shown in Subsection 3.5 that the energy barriers for proton transfer in clusters of different sizes embedded in the PE phase of ADP, are strongly dependent on the O-O distance and the cluster sizes (Fig. 5). This behavior is similar to that found in KDP (see Fig. 4).(47; 48) As in that case, it is expected that the H $\rightarrow$ D substitution in ADP, which implies an increase of the D localization near the potential minimum along the O-O bond, will lead to its weakening and a lattice expansion. The consequent barrier-height increase would couple selfconsistently with tunneling in the way described above leading to the large isotope effect observed in ADP.(62) This mechanism is expected to be universal for the family of H-bonded ferroelectrics exhibiting large isotope effects.

3.7 Additional ab initio results for KDP

3.7.1 Pressure effects

Neutron diffraction experiments under pressure revealed in the late eighties the importance of structural modifications due to deuteration.(4; 62) A remarkable correlation was found between T_c and the separation δ between the two equivalent positions along the H-bond, observed to be occupied by the H(D) atoms. Moreover, the critical temperature T_c of KDP could be almost perfectly reproduced by compressing DKDP in such a way as to bring the value of δ to that of KDP at ambient pressure. Furthermore, T_c appears to be linearly proportional to δ for different H-bonded ferroelectric materials, deuterated or not, all of them ending at a universal point $\delta_0 \approx 0.2$ Å as T_c goes to zero and the FE phase is no longer possible.(62) The experiments then suggest that the effects of deuteration can be reverted by applying pressure. This prompted us to explore the connection between pressure and isotope effects by means of first-principles calculations and the above described phenomenological model. Deuterons, being heavier, have less probability than H to be found near the bond center, where a collective double-well barrier exist (see Fig. 4). Thus they localize farther than H from the bond center (larger δ). One might expect that by applying pressure to DKDP, thus lowering the energy barrier at the bond center, the latter will be approached by the peak of the D probability distribution. For the pressure at which the peak separation δ for DKDP coincides with that of KDP, both would have the same T_c according to the observed phenomenology.(62) Moreover, this T_c equality is observed for any pressure applied to KDP and correspondingly higher pressure applied to DKDP such that their δ's are brought in coincidence. However the δ coincidence at the high pressures used in the experiments is achieved in our calculations only

by taking into account the mutual self-consistent arrangement between D(H) distribution and host structure (the geometrical effect), modeled as explained in Subsection 3.6 at the different imposed pressures. More details on this analysis are given in Refs.(48; 72). These results give further support to our self-consistent model explanation of the geometrical isotope effects.

3.7.2 Structure and energetics of Slater and Takagi defects

The observation by magnetic resonance experiments of deuterons jumping along the bridges in the FE phase of DKDP,(73) allows for the appearance of phosphates with 2 latteral attached D (called Slater defects) or a pair of neighboring phosphates, one with only 1 and the other with 3 attached D's (called Takagi defects, which violate the Ice rules). Slater and Takagi defects have been accounted for in the modeling of domain-walls motion near the transition in KDP and DKDP.(74; 75) The energies of these defects have been estimated from model calculations in several compounds of the KDP-family.(76–79) By means of *ab initio* calculations we had obtained the structure and stability of the Slater and Takagi defects in the FE phase of KDP.(17) We showed that the Slater defects are stabilized only in form of defect chains. In contrast, the Takagi defects are not stable. Our result for the energy necessary to form a Takagi-pair defect is $\approx$ 54 meV, in fair good agreement with previous phenomenological estimations.(76–79) For the determination of the Slater defect energy we had followed two procedures. One of them was just to calculate the energy per phosphate for the meta-stable configuration of the Slater defect chain. We called this the *correlated* Slater defect energy, and it has a value of 5 meV, in good agreement with the phenomenological estimations. The other procedure was to displace the two hydrogens connecting three neighboring phosphates, in such a way to leave two phosphates in Takagi configurations connected to an intermediate phosphate in lateral Slater configuration. This allowed us to obtain an *uncorrelated* Slater defect energy of $\approx$ 17 meV. These results suggest that the phenomenological estimation involve correlations between configurations of different H_2PO_4 groups. We observed that the formation of the Slater defect chains is accompanied by phosphate rotations, and a concomitant lattice contraction in the basal plane. This allowed us to suggest that a lattice contraction observed in the neighborhood of the phase transition (80; 81) can be ascribed to an increase of the Slater defect population.

3.7.3 Developement of an atomistic model

The possibility of studying the FE-PE phase transition at a first-principles level requires the formation of clusters of enough size to enable tunneling, as described in Section 3.4. This is precluded by the required sizes of the simulation supercells, which leads to exceedingly demanding computations. Even more demanding is the consideration of the proton (deuterium) quantum dynamics. Therefore, in order to address these issues we developed an extended shell model of KDP capable of describing reasonably well the physical properties of the system in its different phases.(67; 82) We paid particular attention to those properties that are relevant to the FE-PE phase transition. Fairly good agreement with first-principles and experimental results was achieved for the structural parameters, Γ-phonon frequencies in both the PE and FE phases,(83) and the underlying potential energy for a single H moving along the H-bond in the FE phase.(67) The total energies as a function of global displacements with the FE mode pattern and as a function of local distortions in the PE phase for the various cluster sizes analyzed in Section 3.4 in both KDP and DKDP, are also well reproduced.(82)

4. Discussion and conclusions

The described ab-initio calculations of the PE and ordered equilibrium phases of ADP and KDP lead to structural parameters in good agreement with the experimental data obtained by x-ray and neutron diffraction. The systematic underestimation of the O-O distances compared to experiments in both compounds should be ascribed to the approximation in the exchange-correlation functional. On the other hand, the apparent underestimation of the acid hydrogen off-center distance $\delta/2$ in the calculation for ADP could be ascribed to the unreliability of the x-ray measurements of the proton position. The N-O distance in the N-H$\cdots$O bridges of ADP is very close to the usual value ≈ 2.8 Å for this kind of bonds.(84–86) In addition, a somewhat overestimated N-H distance was found in our calculation when compared to the neutron diffraction measurements. This could be ascribed to the local orbital approximation for the valence electrons used in the SIESTA code. We have observed similar discrepancies between SIESTA and plane wave pseudopotential calculations for KDP in the calculation of the O-H distance in the O-H$\cdots$O bridges.(48)

The FE transition and the nature of the instability that leads to the onset of the spontaneous polarization P_s in KDP have been extensively discussed in the past.(28; 87; 88) It was originally assumed that P_s, which is oriented along the c-axis, was due to the displacements of K^+ and P^- ions along this axis, although the H(D) ordering, nearly parallel to the basal plane, is undoubtedly correlated with the transition.(28) Within this model, the observed value of P_s can only be explained if very large charges for the phosphorus ion are assumed.(87) Another mechanism was that of Bystrov and Popova (87) who proposed that the source of P_s could be the electron density shift in the P-O and P-O-H bonds in the polar direction, which occurs when the protons order almost perpendicularly. However, model calculations cannot determine this assumption for it is originated in the complex electronic interactions in the system.(88)

We were able to overcome this model limitation by means of *ab initio* calculations. Actually, we have shown that the FE instability in KDP has its origin on an electronic charge reorganization within the internal P-O and P-O-H bonds of the phosphates, as the H-atoms order off-center in the H-bonds. The overall effect produced by the H-ordering is an *electronic charge flow* from the O2 side to the O1 side of the PO_4 tetrahedron. This comes with a distortion of the phosphates.(46; 48) The mechanism found agrees with the explanation given in Ref. (87), and is also in accordance with the results obtained by another recent first-principles calculation.(89)

We have found that the charge redistributions in the the acid proton bridges and phosphates associated with the instabilities in ADP and KDP are very similar. In fact, as it happens in KDP, the flow of charge from the O2 side to the O1 side of the PO_4 tetrahedron is also verified in ADP. However, this alone is insufficient to produce antiferroelectricity in ADP, as is shown in an energy analysis of different possible distortions.(21) On the other hand, a differentiation between two types of N-H$\cdots$O bridges, long and short, also occurs concomitant with the ammonium tetrahedra distortions as the AFE instability takes place in ADP. We have also verified by a Mulliken charge analysis the existence of an electronic charge flow from the long to the short N-H$\cdots$O bridges which occurs simultaneously with the ammonium distortion. This charge flow is absent in the hypothetical FE phase of ADP.(60) The above features found in ADP are also confirmed by charge density difference plots.(21)

We have shown that the optimization of the N-H$\cdots$O bridges leads to the stabilization of the AFE phase in ADP. This is consistent with the proposition of Schmidt that an effective

acid-protons interaction mediated by the ammonium through the N-H$\cdots$O bonds plays an important role.(15; 21) Actually, the strengthening of N-H$\cdots$O bonds which generates the energy imbalance in favor of the AFE phase, also distorts the NH_4^+ ion, repels the acid H that is close to the stronger N-H$\cdots$O bond, involves significant charge transfers, and thus creates dipole moments in the plane of the O-H$\cdots$O bonds, in full agreement with the neutron data (23) and Schmidt's conjecture (15).

There is a long controversy regarding the character of the FE transition in KDP. The coupled proton-phonon model displaying essentially a displacive-like transition is supported by some experimental facts.(90) The importance of the order-disorder character of the transition originated in the H_2PO_4 unit dipoles is highlighted by other experiments, e.g. Raman studies.(91; 92) Moreover, electron-nuclear double-resonance (ENDOR) measurements (93) indicate that not only the H_2PO_4 group, but also the K atoms, are disordered over at least two configurations in the paraelectric phase. Neutron scattering experiments show that the P atom is distributed over at least two sites in DKDP. (69; 70) It is clear that, in spite of the still unresolved character of the transition, local instabilities arising from the coupling of light and heavy ions are very important in this system. This should be the case, irrespective of the correlation length scale associated with the transition.

Our calculations in the PE phase of KDP showed that local proton distortions with the FE mode pattern (Fig. 2) need to be accompanied by heavy ion relaxations in the PO_4-K group in order to produce significant instabilities,(47; 48) a fact which is in agreement with experiments.(69; 70; 91–93) The correlation length associated with the FE instability is much larger in KDP than in DKDP, suggesting that DKDP will behave more as an order-disorder ferroelectric than KDP. We have also demonstrated the relevance of proton correlations and the acid H-bond geometry in the energy scale of the local AFE instabilities inherent to the PE phase of ADP.(60) This fact is found to be similar to that observed in KDP.

Undoubtedly, the huge isotope effect in the critical temperature and the order parameter of the transition is the most striking feature not yet satisfactorily understood in these compounds. As we have already mentioned, the first explanation was that proposed by the tunneling model and later modifications.(27; 28) However, the vast set of experiments later carried out by Nelmes and co-workers, (4; 10; 38; 62; 69; 70) and the comprehensive structural compilation done by Ichikawa *et al.*, (3; 36; 40) showed the importance of the so-called geometrical effect as an alternative explanation. An overall and consistent explanation of the phenomenon became more elusive when other experiments (34; 35; 91; 92; 94) and models (29; 30; 32; 33; 41; 43; 95) favored one or the other vision, or even both. Still unanswered questions like: if tunneling occurs, what are the main units that tunnel?, what is the connection between tunneling and geometrical effects?, and what is the true microscopic origin of the latter?, are possibly some of the reasons why a full explanation of the isotope effect is not yet available. In the present review, we showed how the *ab initio* scheme have also helped to shed light onto the underlying microscopic mechanism for the isotope effect.

We demonstrated in KDP that protons alone are not able to tunnel. In fact, distortions involving only the light atoms display tiny double wells, and the particles are broadly delocalized around the center of the H-bonds. We concluded that the simplified version of the tunneling model, i.e. that of a tunneling proton, or even a collective proton soft-mode alone, is not supported by our calculations.

Due to the correlation with heavier ions, we observe "tunneling clusters" with an effective mass much larger than that of a single, or even several, protons (deuterons). The different sizes

of these clusters correspond to different lengths and energy scales whose magnitudes differ between KDP and DKDP and which compete in their PE phases. This view agrees with recent neutron Compton scattering experiments where it is concluded that there is a mass-dependent quantum coherence lenght in these compounds.(94) We found that the smallest tunneling unit in DKDP is the KD_2PO_4 group. This is in accordance with the idea developed by Blinc and Žekš of a tunneling model for the whole H_2PO_4 unit,(96) which helped to describe the typical order-disorder phenomena observed in some experimental trends.(90) However, as we reviewed in this work, the explanation for the isotope effect is even more complex than the concept of an atom or molecular unit that is able to tunnel alone as its main cause.

It is clear that the larger clusters will prevail as the transition approaches, in spite of the complex scenario existing in the PE phase due to the appearance of different length scales. We showed that tunnel splittings in these clusters at fixed potential are much smaller than the thermal energy at the critical temperature. Thus, if the potential remains fixed, tunneling alone is not able to account for the large isotope effect in the system. However, the main effect of replacing deuterons by protons is an enhancement of the quantum delocalization at the bond center, which affects the chemical properties of the O-H$\cdots$O bond. This in turn shrinks the lattice which further delocalizes the proton, and so on in a nonlinear loop.

We have shown with a simple model based on our *ab initio* results, how this feedback effect strongly amplifies the geometrical modifications in the H(D)-bridge. The selfconsistent phenomenon is triggered by tunneling, but, in the end, the geometrical effect dominates the scenario and accounts for the huge isotope effect, in agreement with neutron scattering experiments. (4; 62) Therefore, these aspects, which were largely debated in the past, here appear as complementary and deeply connected to each other. (29; 30; 47; 48; 88)

The existence of tunneling units has been found in a large variety of molecular compounds and biomolecules. Moreover, the importance of both, tunneling and structural changes, has been well established in the reaction mechanisms of enzymes (97) and other biological processes. It is clear that the nonlinear feedback between tunneling and structural modifications, as discussed in this review, is a phenomenon of wider implications. As one of the numerous examples where these features are observed, one can mention the FE transition in $CaAl_2Si_2O_7(OH)_2H_2O$ (lawsonite), which was recently shown to be related to the proton mobility.(98) Actually, the much smaller isotope effect observed for this compound in comparison with that for KDP seems to be related with the absence of strong correlations with the host, which are essential for the nonlinear mechanism discussed above.(47; 48; 98) Therefore, our results for the H-bonded ferroelectrics support the conclusion that the general theories of host-and-tunneling systems must be revised. (5)

We would now like to extend our methodology to different systems like the subset of systems known as the 'proton glasses' in which an alloy is made by mixing a ferroelectric compound with an isomorphic antiferroelectric compound.(99; 100) These materials show the slow dynamics of a glassy system, even though they are single crystals, and exhibit the H-D isotope effect.(99; 100) Other interesting systems are those where the transitions could be classified either of 'order-disorder' or 'displacive' type or where the order-disorder and the displacive behaviors coexist.(33) In recent studies of the hydrogen-bonding properties of the NH_4^+ cation, ferroelectricity was discovered in a new class of magnetic compounds $M_{3-x}(NH_4)_xCrO_8$ (M = Na, K, Rb, Cs).(101) It was found that the transition is of the order-disorder type, with a critical temperature depending linearly on the composition variable x. This suggests that the N-H$\cdots$O bond plays the central role in the FE instability of these new compounds, with a

net effect reminiscent of the mechanism found in ADP,(21) although in the latter the AFE ordering is favored. Ferroelectric properties were also recently found in a related novel ammonium-based compound, Diammonium Hypodiphosphate $(NH_4)_2H_2P_2O_6$, although there is not yet a theoretical microscopic explanation of this phenomenom.(102) Therefore, it would be also desirable to extend our first-principles calculations to the study and dessign of new FE and AFE materials based on the H-bonding properties of the NH_4^+ cation.

On the other hand, a promising perspective arises from the recently developed atomistic model for KDP,(67) which was briefly described in subsection 3.7.3. As mentioned above, it was fitted to reproduce first-principles structural, dynamical and energetic properties of various stable and metastable structures to a very good extent.(67) This model will be useful to study, in large systems, the nuclear quantum-dynamical and thermal fluctuations responsible for the FE-PE phase transition and the isotope effects observed in KDP.

In summary, it has been shown that the H off-centering controls the instability proccess in KDP. This ordering leads to an electronic charge redistribution and ionic displacements that originate the spontaneous polarization of the FE phase. On the other hand, the origin of antiferroelectricity in ADP is ascribed to the optimization of the N-H$\cdots$O bonds. The closeness in energy found between the AFE and the hypothetical FE phases in ADP is in accordance with the experimental observation of coexistence of AFE and FE microdomains near the vicinity of the transition. The dynamics of protons alone in the PE phases of KDP and ADP cannot explain the observed double-peaked proton distribution in the bridges. By contrast, the importance of the correlations between protons and heavier ions displacements within clusters has been demonstrated. Recent evidence of tunneling obtained from Compton scattering measurements supports our conclusions regarding the existence of tunneling clusters. We have also shown that the huge isotope effect observed in KDP cannot be explained by the quantum effects of a mass change obtained in a system at fixed geometry and potential. We found that as a consequence of the modification of the covalency in the bridges, structural changes arise producing a feedback effect on the tunneling that strongly enhances the phenomenon. The resulting amplification in this nonlinear feedback of the geometrical effect is in agreement with experimental data from neutron scattering.

5. Acknowledgements

We thank E. Tosatti, G. Colizzi, and A. Bussmann-Holder for helpful discussions. S. K., J. L., and R. L. M. acknowledge support from Consejo Nacional de Investigaciones Científicas y Técnicas (CONICET), Argentina.

6. References

[1] *Proton Transfer in Hydrogen-Bonded Systems*; NATO ASI Series B: Physics, Vol. 291; Ed. T. Bountis; Plenum Press (1992); ISBN 0-306-44216-7.
[2] J.M. Robertson and A.R. Ubbelohde, Proc. R. Soc. London A 170, 222 (1939).
[3] M. Ichikawa, Chem. Phys. Lett. 79, 583 (1981).
[4] M.I. McMahon, R.J. Nelmes, W.F. Kuhs, R. Dorwarth, R.O. Piltz, and Z. Tun, Nature (London) 348, 317 (1990).
[5] J.A. Krumhansl, Nature (London) 348, 285 (1990).
[6] M. E. Lines and A. M. Glass, *Principles and Applications of Ferroelectric and Related Materials* (Clarendon Press, Oxford, 1977).

[7] G. Busch and P. Scherrer, Naturwiss. 23, 737 (1935).
[8] G. Busch, Helv. Phys. Acta 11, 269 (1938).
[9] R. Blinc and B. Žekš, in *Soft Modes in Ferroelectrics and Antiferroelectrics*, edited by E. P. Wohlfarth (North-Holland, Amsterdam, 1974).
[10] R. J. Nelmes, Ferroelectrics 71, 87 (1987).
[11] Y. Takagi, Ferroelectrics 72, 67 (1987).
[12] F. Gervais and P. Simon, Ferroelectrics 72, 77 (1987).
[13] G. Samara, Ferroelectrics 71, 161 (1987).
[14] J. C. Slater, J. Chem. Phys. 9, 16 (1941).
[15] V. H. Schmidt, Ferroelectrics 72, 157 (1987).
[16] Y. Takagi, J. Phys. Soc. Jpn. 3, 273 (1948).
[17] J. Lasave, S. Koval, N. S. Dalal, and R. Migoni, Phys. Rev. B 72, 104104 (2005).
[18] T. Nagamiya, Progr. Theor. Phys. 7, 275 (1952).
[19] Y. Ishibashi, S. Ohya, and Y. Takagi, J. Phys. Soc. Jpn. 33, 1545 (1972).
[20] Y. Ishibashi, S. Ohya, and Y. Takagi, J. Phys. Soc. Jpn. 37, 1035 (1974).
[21] J. Lasave, S. Koval, N.S. Dalal, and R.L. Migoni, Phys. Rev. Lett. 98, 267601 (2007).
[22] S. Havlin, E. Litov, and H. Sompolinsky, Phys. Rev. B 14, 1297 (1976).
[23] A. W. Hewat, Nature 246, 90 (1973).
[24] V. H. Schmidt, J. T. Wang, and P. Schnackenberg, Jpn. J. Appl. Phys. 24, Suppl. 24-2, 944 (1985).
[25] B. Lamotte, J. Gaillard and O. Constantinescu, J. Chem. Phys. 57, 3319 (1972).
[26] N.S. Dalal, J.A. Hebden, D.E. Kennedy and C.A. McDowell, J. Chem. Phys. 66, 4425 (1977).
[27] R. Blinc, J. Phys. Chem. Solids 13, 204 (1960).
[28] K. Kobayashi, J. Phys. Soc. Jpn. 24, 497 (1968).
[29] E. Matsushita and T. Matsubara, Prog. Theor. Phys. 67, 1 (1982).
[30] T. Matsubara and E. Matsushita , Prog. Theor. Phys. 71, 209 (1984).
[31] M. Kojyo and Y. Onodera, J. Phys. Soc. Jpn. 57, 4391 (1988).
[32] A. Bussmann-Holder and K. H. Michel, Phys. Rev. Lett. 80, 2173 (1998).
[33] N. Dalal, A. Klymachyov and A. Bussmmann-Holder, Phys. Rev. Lett. 81, 5924 (1998).
[34] G.F. Reiter, J. Mayer and P. Platzman, Phys. Rev. Lett. 89, 135505 (2002).
[35] S. Ikeda, Y. Noda, H. Sugimoto and Y. Yamada, J. Phys. Soc. Jpn. 63, 1001 (1994).
[36] M. Ichikawa, K. Motida and N. Yamada, Phys. Rev. B 36, R874 (1987).
[37] Z. Tun, R.J. Nelmes, W.F. Kuhs and R.D.F. Stansfield, J. Phys. C 21, 245 (1988).
[38] R.J. Nelmes, J. Phys. C 21, L881 (1988).
[39] J. Seliger and V. Žagar, Phys. Rev. B 59, 13505 (1999).
[40] M. Ichikawa, D. Amasaki, T. Gustafsson and I. Olovsson, Phys. Rev. B 64, R100101 (2001).
[41] H. Sugimoto and S. Ikeda, Phys. Rev. Lett. 67, 1306 (1991).
[42] H. Sugimoto and S. Ikeda, J. Phys.: Condens. Matter 8, 603 (1996).
[43] D. Merunka and B. Rakvin, Phys. Rev. B 66, 174101 (2002).
[44] D. Merunka and B. Rakvin, Solid State Commun. 129, 375 (2004).
[45] D. Merunka and B. Rakvin, Chem. Phys. Lett. 393, 558 (2004).
[46] S. Koval, J. Kohanoff, R. L. Migoni, and A. Bussmann-Holder, Comput. Mater. Sci. 22, 87 (2001).
[47] S. Koval, J. Kohanoff, R. L. Migoni and E. Tosatti, Phys. Rev. Lett. 89, 187602 (2002).

[48] S. Koval, J. Kohanoff, J. Lasave, G. Colizzi, and R.L. Migoni, Phys. Rev. B 71, 184102 (2005).
[49] P. Hohenberg and W. Kohn, Phys. Rev. 136, B864 (1964).
[50] W. Kohn and L. J. Sham, Phys. Rev. 140, A1133 (1965).
[51] P. Ordejón, E. Artacho and J.M. Soler, Phys. Rev. B 53, R10441 (1996).
[52] D. Sánchez-Portal, P. Ordejón, E. Artacho and J.M. Soler, Int. J. Quantum Chem. 65, 453 (1997).
[53] O.F. Sankey and D.J. Niklewski, Phys. Rev. B 40, 3979 (1989).
[54] N. Troullier and J.L. Martins, Phys. Rev. B 43, 1993 (1991).
[55] J.P. Perdew, K. Burke and M. Ernzerhof, Phys. Rev. Lett. 77, 3865 (1996).
[56] D. R. Hamann, Phys. Rev. B 55, R10157 (1997).
[57] A. D. Becke, Phys. Rev. A 38, 3098 (1988).
[58] C. Lee, W. Yang, and R. Parr, Phys. Rev. B 37, 785 (1988).
[59] M. Tuckerman, D. Marx and M. Parrinello, Nature 417, 925 (2002).
[60] J. Lasave, S. Koval, R. L. Migoni, and N. S. Dalal, unpublished.
[61] R.J. Nelmes, Z. Tun and W.F. Kuhs, Ferroelectrics 71, 125 (1987).
[62] R. J. Nelmes, M. I. McMahon, R. O. Piltz and N. G. Wright, Ferroelectrics 124, 355 (1991).
[63] A. R. Grimm, G. B. Bacskay and A. D. J. Haymet, Mol. Phys. 86, 369 (1995).
[64] T. R. Dyke, K. R. Mack and J. S. Muenter, J. Chem. Phys. 66, 498 (1977).
[65] T. Fukami, S. Akahoshi, K. Hukuda, and T. Yagi, J. Phys. Soc. Jpn. 56, 2223 (1987).
[66] N. Pérès, M. Souhassou, B. Wyncke, G. Gavoille, A. Cousson, and W. Paulus, J. Phys.: Condens. Matter 9, 6555 (1997).
[67] J. Lasave, J. Kohanoff, R. L. Migoni, and S. Koval, Physica B 404, 2736 (2009).
[68] G. Colizzi, PhD Thesis (Queen's University Belfast, 2005).
[69] M. I. McMahon, R. J. Nelmes, R. O. Piltz and W. F. Kuhs, Europhys. Lett. 13, 143 (1990).
[70] M. I. McMahon, R. J. Nelmes, R. O. Piltz, W. F. Kuhs and N. G. Wright, Ferroelectrics 124, 351 (1991).
[71] G. A. Samara, Ferroelectrics 5, 25 (1973).
[72] G. Colizzi, J. Kohanoff, J. Lasave, S. Koval and R.L. Migoni, Ferroelectrics 301, 61 (2004).
[73] V.H. Schmidt and E.A. Uehling, Phys. Rev. 126, 447 (1962).
[74] V.H. Schmidt, Phys. Rev. 164, 749 (1967).
[75] V.H. Schmidt, G. Bohannan, D. Arbogast and G. Tuthill, J. Phys. Chem. Solids 61, 283 (2000).
[76] H.B. Silsbee, E.A. Uehling, and V.H. Schmidt, Phys. Rev. 133, A165 (1964).
[77] R. Blinc and S. Svetina, Phys. Rev. 147, 430 (1966).
[78] W. Reese, Phys. Rev. 181, 905 (1969).
[79] C.W. Fairall and W. Reese, Phys. Rev. B 11, 2066 (1975).
[80] J. Kobayashi, Y. Mesu, I. Mizutani, and Y. Enomoto, Phys. Status Solidi A 3, 63 (1970).
[81] A. Katrusiak, Phys. Rev. B 48, 2992 (1993).
[82] S. Koval, J. Lasave, J. Kohanoff and R. Migoni, Ferroelectrics 401, 103 (2010).
[83] G. Colizzi, J. Kohanoff, J. Lasave, and R. L. Migoni, Ferroelectrics 401, 200 (2010).
[84] A. E. Mirsky and L. Pauling, Proc. Nat. Acad. Sci. 22, 439 (1936).
[85] S. Scheiner in *Proton Transfer in Hydrogen-Bonded Systems*, NATO ASI Series B: Physics, Vol. 291, Ed. T. Bountis, p. 29 (Plenum, 1992).
[86] L. Pacios in *Hydrogen Bonding - New Insights*, Ed. S. J. Grabowski, p. 109 (Springer, 2006).
[87] D. S. Bystrov and E. A. Popova, Ferroelectrics 72, 147 (1987).

[88] R. Blinc and B. Žekš, Ferroelectrics 72, 193 (1987).
[89] Q. Zhang, F. Chen, N. Kioussis, S. G. Demos and H. B. Radousky, Phys. Rev. B 65, 024108 (2001).
[90] See for instance, M. Tokunaga and T. Matsubara, Ferroelectrics 72, 175 (1987); and references therein.
[91] Y. Tominaga, M. Kasahara, H. Urabe and I. Tatsuzaki, Solid State Commun. 47, 835 (1983).
[92] Y. Tominaga, H. Urabe and M. Tokunaga, Solid State Commun. 48, 265 (1983).
[93] B. Rakvin and N. S. Dalal, Phys. Rev. B 44, R892 (1991).
[94] G. Reiter, A. Shukla, P. M. Platzman and J. Mayers, New J. Phys. 10, 013016 (2008).
[95] S. E. Mkam Tchouobiap and H. Mashiyama, Phys. Rev. B 76, 014101 (2007).
[96] R. Blinc and B. Žekš, J. Phys. C15, 4661 (1982).
[97] A. Kohen, R. Cannio, S. Bartolucci and J. P. Klinman, Nature 399, 496 (1999).
[98] E. K. H. Salje and M. A. Carpenter, J. Phys.: Condens. Matter 23, 112208 (2011).
[99] N.S. Dalal and A. Bussmann-Holder, Structure and Bonding, 24, 1 (2006).
[100] Z. Trybulla, J. Stankowski, L. Szczepanska, R. Blinc, A. I. Weiss, and N.S. Dalal, Physica B 153, 143 (1988).
[101] R. Samantaray, R. J. Clark, E. S. Choi, H. Zhou, and N. S. Dalal, J. Am. Chem. Soc. 133, 3792 (2011).
[102] P. Szklarz, M. Chański, K. Ślepokura and T. Lis, Chem. Mater. 23, 1082 (2011).

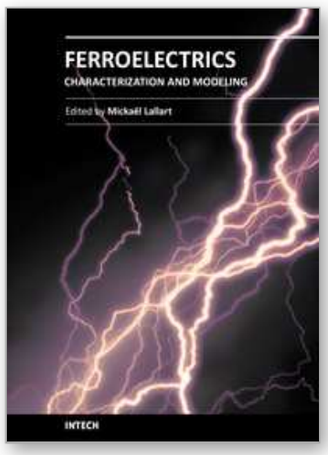

Ferroelectrics - Characterization and Modeling

Edited by Dr. MickaÃ«l Lallart

ISBN 978-953-307-455-9
Hard cover, 586 pages
Publisher InTech
Published online 23, August, 2011
Published in print edition August, 2011

Ferroelectric materials have been and still are widely used in many applications, that have moved from sonar towards breakthrough technologies such as memories or optical devices. This book is a part of a four volume collection (covering material aspects, physical effects, characterization and modeling, and applications) and focuses on the characterization of ferroelectric materials, including structural, electrical and multiphysic aspects, as well as innovative techniques for modeling and predicting the performance of these devices using phenomenological approaches and nonlinear methods. Hence, the aim of this book is to provide an up-to-date review of recent scientific findings and recent advances in the field of ferroelectric system characterization and modeling, allowing a deep understanding of ferroelectricity.

InTech Europe
University Campus STeP Ri
Slavka Krautzeka 83/A
51000 Rijeka, Croatia
Phone: +385 (51) 770 447
Fax: +385 (51) 686 166
www.intechopen.com

InTech China
Unit 405, Office Block, Hotel Equatorial Shanghai
No.65, Yan An Road (West), Shanghai, 200040, China
中国上海市延安西路65号上海国际贵都大饭店办公楼405单元
Phone: +86-21-62489820
Fax: +86-21-62489821

IntechOpen